ANISOTROPIC GEOTHERMAL HOST ROCK? CASE STUDY OF NEVADO DEL RUIZ, COLOMBIA

Pablo Aguilera[1,3] and Ludmila Adam[1]

[1] School of Environment, University of Auckland, Auckland, New Zealand

[3]Colombian Geothermal Association, Bogotá, Colombia

pablo.aguilera@auckland.ac.nz

Keywords: *Anisotropy, Colombia, metamorphic rocks, Nevado del Ruiz, ultrasonic waves.*

ABSTRACT

To date, geothermal exploration at Nevado del Ruiz (NRV) volcano suggests that metamorphic formations are the possible hosts of a geothermal reservoir. Measurements of ultrasonic elastic waves on metamorphic rock samples collected from outcrops and the well Nereidas-1 at in-situ pressure conditions. We find that elastic wave anisotropic is influenced by foliation and vein hydrothermal alteration at all effective pressures of interest. The presence of elastic wave anisotropy is crucial to correct seismic travel times for earthquake location, seismic tomography, monitoring, and design of future geothermal boreholes.

1. INTRODUCTION

The NRV geothermal field is located in a sector known as "Valle de Nereidas" in the municipality of Villamaria – Caldas. This area is near the city of Manizales, approximately 150 km west of the Colombian capital city Bogotá. The elevation of the field range between 3200 and 3600 meters above sea level. 2D numerical modeling of heat transfer at reservoir scale and rock thermal conductivity of the Cajamarca Group suggests a geothermal potential range between 54 MWt and 130 MWt (Velez et al., 2018).

Geothermal site characterization shows that the geological formation known as The Cajamarca Complex, a metamorphic rock formation comprised mainly of schists, is the host of a hydrothermal reservoir (Monsalve et al. 1998) (Figure 1). The presence of approximately 200 ºC at 1500 meters depth has been proven by the well Nereidas-1. Geothermal gradient wells of 300 m and 240 m depth estimated temperature gradients between 160 ºC/km and 200 ºC/km (Rojas, 2012). The geochemistry on surface hot springs and fumaroles indicates greater possible temperatures of up to 260 ºC at the reservoir level (Alfaro et al., 2002; Alfaro et al., 2005). A 3D conceptual model of NRV (González-García et al., 2015) consisting of a convective hydrothermal system that interacts with the magmatic flow that ascends through a tripartite system of magmatic chambers (Giggenbach et al., 1990; Londono et al., 2018; Lundgren et al., 2015; Vargas et al., 2017, Cervantes, 2019). The flow pattern of the hydrothermal fluids is structurally controlled by the faults of Nereidas, Rio Claro, Santa Rosa, Samaná Sur and the discontinuity of the prevolcanic basement facilitating superficial manifestations of sulphide, chloride and bicarbonate waters (Mejía et al., 2012; Moreno et al., 2018). Likewise, advanced argillic alteration has caused a clay cap that restricts the circulation of hydrothermal fluids (Forero, 2012).

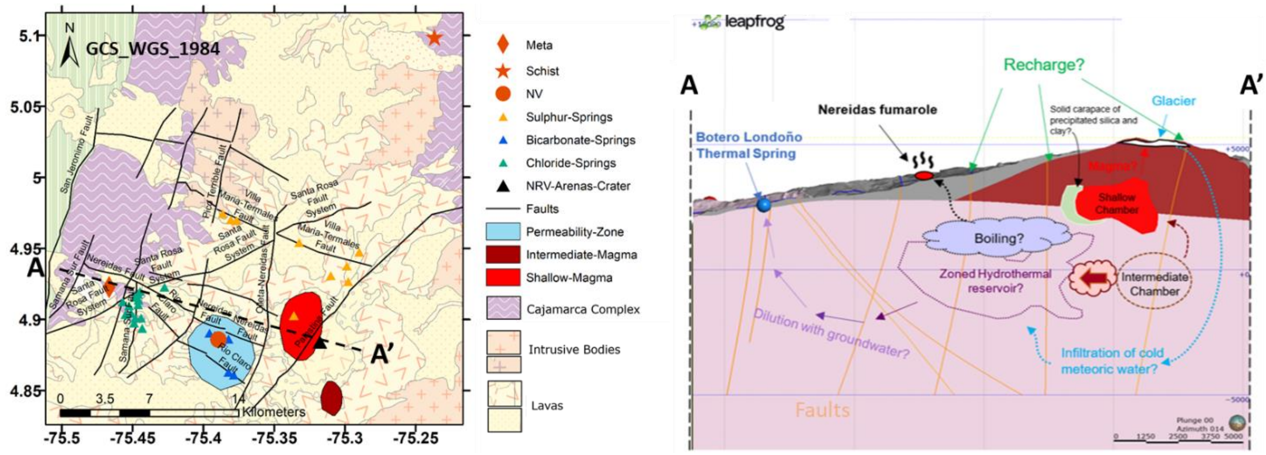

Figure 1: Left: Location of NRV geothermal area. Rock samples are labeled as Meta, Schist and NV. The permeability zone is suggested by Cervantes, 2019 as the location of the geothermal reservoir. Right: Conceptual model of NRV geothermal system from the A-A' cross-section suggested by Cervantes, 2019.

Metamorphic rocks are known to have high seismic wave speed anisotropy induced by foliation, mineral composition, and fractures (Adam et al., 2020; Johnson et al., 1974). The aim of this work is to characterize and quantify the elastic wave anisotropy of NRV metamorphic host through lab ultrasonic measurements and petrographic descriptions. The outcomes will be significant not only for improving the imaging the NRV geothermal host rock but also for the upcoming well-drilling campaign.

2. METHODOLOGY

Metamorphic rock samples from the NRV were collected mostly from outcrops. Thin section petrography, XRD analysis and P- and S- waves ultrasonic measurements at room conditions and under subsurface effective pressure were carried out on the rock samples. By comparing wave speed propagation at different directions to foliation, the elastic wave anisotropy of the samples is characterized and interpreted in the context of the microstructural and mineralogical information.

2.1 Samples

Three metamorphic rock samples were collected at the locations specified in Figure 1. Core samples with a 25 mm diameter were extracted from the field samples. Based on visual identification, the axis of the core cylinder is drilled parallel to foliation. As they come from different locations, samples are labelled as "NV", "Schist" and "Meta."

The sample NV comes from the well Nereidas-1 from a depth of 1225 m. Monsalve et al. (1998) described the lithology at this depth as a calcsilicate gneiss with the presence of epidote, sericite, and calcite as secondary minerals. At this depth, a thermometamorphic zone is identified, resulting in propylitic alteration. Our thin section petrography and XRD analysis on NV indicates the major minerals are andradite and quartz. Minor components are epidote, unidentified opaque and feldspar minerals (possibly K-feldspar), and chlorite is present only as a trace. We identify this sample as an andradite garnet. Microphotographs allows us to visualize the vein alteration of this sample (Figure 2).

The samples Schist and Meta were collected from outcrops where the Cajamarca Complex is exposed according to the geological map from the Colombian Geological Survey described by Tapias et al. (2017). Thin section petrography and XRD analysis indicate the sample Schist contains chlorite, mica, and quartz as major trace minerals. The foliation in this sample is clearly identified in the microphotographs as is shown in Figure 2. We interpret this this sample is a greenschist. The sample Meta is composed of chlorite and quartz as a major mineral, with albite, K-feldspar and plagioclase as minor trace minerals. There is no evidence of foliation through the microphotograph analysis. However, foliation can be observed macroscopically. We interpret this sample as a meta-sandstone.

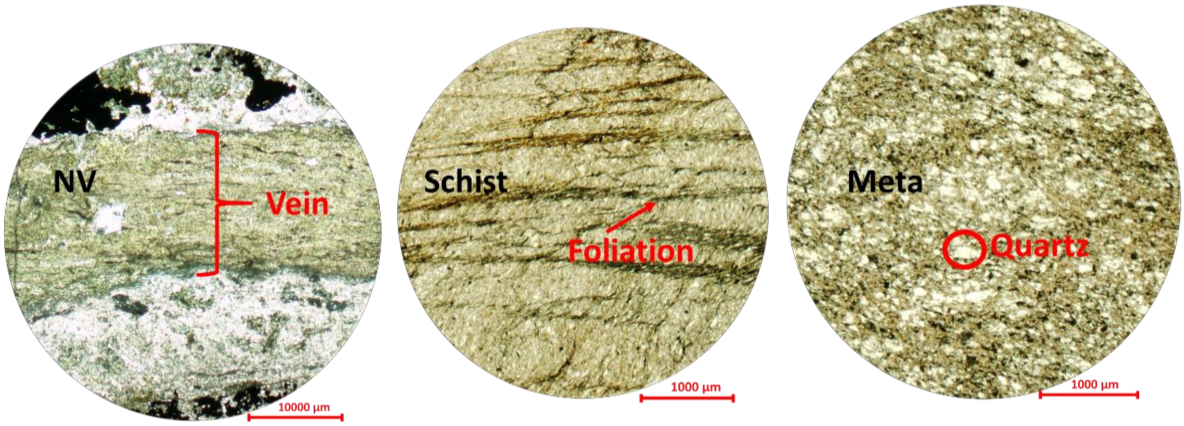

Figure 2: Microphotographs of the metamorphic host rock samples.

2.2 Ultrasonic Measurements

Figure 3 is a sketch of the experimental transducer setup used to acquire P- and S-waves. The source and receiver transducers are aligned on opposite sides of the sample. At room conditions, ultrasonic waves are acquired on cores that have the cylinder axis aligned with the foliation. P- and S-wave data is acquired every 15 degrees. Rock samples under effective pressure are acquired on the plug faces (Figure 3). P- and the S-waves -fast (SH) and slow (SV)- are acquired for pressures from atmospheric to up to 69 MPa. SH and SV are defined as S-waves with particle motion parallel and perpendicular to the foliation plane, respectively (Figure 3 - left). First arrival times are acquired following a dynamic time-warping algorithm by Durán et al. (2019). With these times and the knowledge of sample length, wave velocities are estimated with the corresponding errors.

Proceedings 43rd New Zealand Geothermal Workshop
23-25 November 2021
Wellington, New Zealand
ISSN 2703-4275

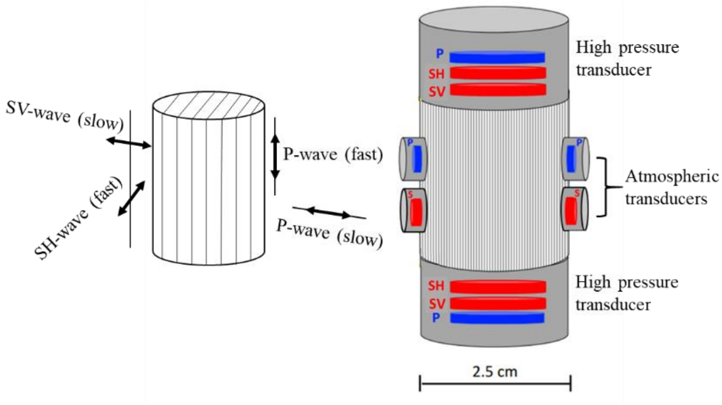

Figure 3: Left: Definitions of fast and slow P- and S-waves modified from Saxena et al. (2018). Right: Laboratory setup for atmospheric and high-pressure ultrasonic measurements modified from Adam et al. (2020).

3. RESULTS

Figure 4 shows P- and S- wave speeds as a function of propagation angle based on transducer ultrasonic measurements at atmospheric conditions. We observed a wave speed symmetry with direction, where fastest P-wave velocities are for waves traveling parallel to the foliation for samples Schist and Meta and to the orientation of the vein of NV, while the slowest velocities are for perpendicular propagation to foliation/vein. For the S-wave the interpretation is similar, but it is the particle motion direction (parallel or perpendicular) to foliation which defined fast and slow S-wave velocity. All samples show velocity dependence with angle that agrees with vertical foliation in the core samples (as sketched in Figure 3). The borehole sample NV has the highest P- and S-wave speeds, probably due to pervasive hydrothermal mineralization with pores and fractures.

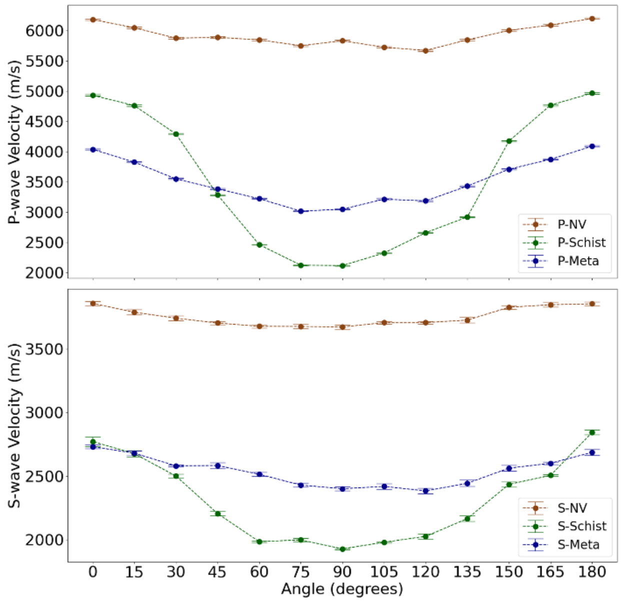

Figure 4: Angle-dependence to rock foliation of P-waves (top) and S-waves (bottom) velocities. At 0 degrees propagation is parallel to foliation/vein, while at 90 degrees propagation is perpendicular to these.

Figure 5A are S-wave velocities parallel (SH) and perpendicular (SV) to foliation and vein alteration for increasing effective pressure. A small non-linear increase in S-wave speeds occurs for the first 10 MPa for the three samples. S-wave anisotropy in the NV and Meta samples shows minor changes below 10 MPa, and behaving mostly pressure insensitive for higher effective pressures, with average S-wave anisotropic values of 3.0% to 7.3% for NV and Meta, respectively. S-anisotropy for the sample Schist is greater than for the other samples and significantly decreasing with effective pressure from 26.0% to 18.2%. Similar to S-waves, the P-wave velocities show an increase with effective pressure (Figure 6).

The increase in P- and S-wave speeds in these samples, point at the presence of natural and coring-induced microfractures (Adam et al. 2020). However, the presence of such fractures has not been observed in the sample microphotographs, either because they are below the microscope resolution or have not been sampled within the volume of the thin section.

In these samples, anisotropy is probably due to mineralized veining (NV), foliation (Meta and Schist), intrinsically anisotropic micas (Schist) and aligned micro-fracturing (Schist). Interestingly, sample Meta shows wave behavior in agreement to a foliated sample. Wave speeds are relatively low suggesting open pore space. However, the lack of pressure dependence of anisotropy in the Meta sample suggests that this pore space not composed of aligned fractures but rather either randomly oriented fractures or high-aspect ratio pores (Charoensawan et al., 2021). On the other hand, the decrease in anisotropy in the Schist sample with effective pressure suggests the presence of foliation-aligned fractures. Although microimages have not been able to image such microfractures, wave speeds are an excellent tool, as waves sense all sizes and orientations of fractures, within the core scale and increase at low pressures (Figure 5A and 6).

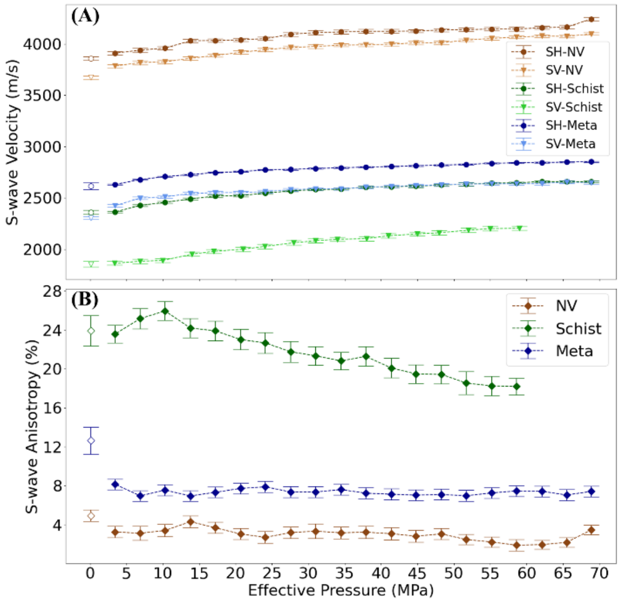

Figure 5: A: Ultrasonic S-wave velocity measurements atmospheric room (open markers) and effective pressure (solid markers). B: S-wave anisotropy atmospheric room (open markers) and effective pressure (solid markers).

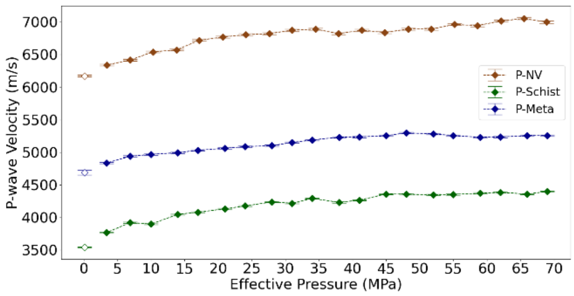

Figure 6: P-wave with pressure. Ultrasonic P-wave velocity measurements atmospheric room (open markers) and effective pressure (solid markers).

4. CONCLUSION

We have estimated P- and S- wave velocities as a function of propagation angle to foliation for three different rock samples associated with the metamorphic geothermal host rock of NRV. We found that there is an anisotropic elastic wave behavior of all of these rocks due to foliation and vein alteration. The P- an S- wave are fastest when travelling parallel to the foliation, vein planes and possibly aligned fractures. Although the slowest wave velocities occur perpendicular to the fastest, more data needs to be acquired in other propagation directions to confirm if the rocks have a transversely isotropic or other kind of symmetry.

Measured P- and S- waves under confining pressure have a non-linear increase for pressures below 10 MPa, possibly due to natural or coring induced microfractures. However, we found that the sample Schist has the highest level of S-wave anisotropy that can be attributed to its high foliation intensity and highly possible aligned microfractures (not evidence at the microphotographs but sensed by the increase of the wave speeds at low pressures). On the other hand, although vein foliation and mineral composition influenced the anisotropic behavior of P- and S- waves, in the measurements carried out for this paper, the anisotropy is non-sensitive to the increase of effective pressure for the one core extracted from the borehole.

We can then conclude from the results of this work that elastic anisotropy will probably play an important role in the geothermal system and cannot be ignored while carrying out exploration activities such as building velocities models for earthquake hypocenter location, seismic tomography or determining well-drilling orientations in metamorphic rocks of NRV.

ACKNOWLEDGEMENTS

Thanks to The SGC for the support on the fieldwork. Ministry of Foreign Affairs and Trade (MFAT) New Zealand development scholarship is acknowledged for the funding offered to the main author for his doctorate studies in New Zealand. We also thank Phil White from PandaGeoscience, Michael Rowe and Andrés Arcila from The University of Auckland for help with the thin sections and XRD analysis.

REFERENCES

Adam. L., Frehner, M., Sauer, K., Toy, V., and Guerin-Marthe, S.: Seismic anisotropy and its impact on imaging the Alpine Fault: an experimental and modeling perspective. Journal of Geophysical Research: Solid Earth, 125. (2020).

Alfaro, C., Aguirre, A., and Jaramillo, L.F.: Inventario de Fuentes Termales Naturales en el Parque Nacional Natural de los Nevados. Technical Report, INGEOMINAS, Bogotá. pp. 60-67. (2002).

Alfaro, C., Velandia, F., and Cepeda, H.: Colombian Geothermal Resources. Proceedings. World Geothermal Congress, Antalya, Turkey. (2005).

Durán, E., Adam, L., and Wallis, I. A robust methodology for time picking and error analysis of ultrasonic waveforms and rock densities in the laboratory. Geophysics. 84. pp. 1-13. (2019).

Charoensawan, J., Adam, L., Ofman, M., Toy, V., Simpson, J., Zhong, X. and Schuck, B.. Fracture shape and orientation contributions to P-wave velocity and anisotropy of Alpine Fault Mylonites. Frontiers in Earth Science, 9, pp. 238. (2021).

Cervantes, C.: 3D Modelling of Faulting and Intrusion of the Nevado del Ruiz Volcano, Colombia, MSc thesis, Reykjavik University, Iceland. (2019).

Forero, J. A.: Caracterización de las Alteraciones Hidrotermales en el Flanco Noroccidental del Volcán Nevado del Ruiz, Colombia, Universidad Nacional de Colombia – Master Thesis, (2012).

Giggenbach, W., García P, N., Londoño C, A., Rodriguez, L., V, Rojas G, N., and Calvache, M., V.: The Chemistry of Fumarolic Vapor and Thermal-Spring Discharges from the Nevado del Ruiz Volcanic-Magmatic-Hydrothermal System, Colombia. Journal of Volcanology and Geothermal Research, **42**(1). pp. 13–39. (1990).

González-García, J., Hauser, J., Annetts, D., Franco, J., Vallejo, E., Regenauer-Lieb, K.: Nevado Del Ruiz Volcano (Colombia): A 3D model combining geological and geophysical information. Proceedings World Geothermal Congress, Melbourne. (2015).

Johnson, L. R., Wenk, H.-R. Anisotropy of physical properties in metamorphic rocks. Tectonophysics, 23(1–2). pp. 79-98. (1974).

Londono, J. M., and Kumagai, H. 4D seismic tomography of Nevado del Ruiz Volcano, Colombia, 2000-2016. Journal of Volcanology and Geothermal Research. 358. pp. 156–168. (2018).

Lundgren, P., Samsonov, S.V., López Velez, C.M.,and Ordoñez, M. Deep source model for Nevado del Ruiz Volcano, Colombia, constrained by interferometric synthetic aperture radar observations. Geophys. Res. Lett. 42. pp. 4816-4823. (2015).

Mejía, E. L., Velandia, F., Zuluaga, C. A., López, J., and Cramer, T.: Análisis estructural al noreste del volcán Nevado del Ruiz, Colombia - aporte a la exploración geotérmica. Boletín De Geología UIS. 34. pp. 27-41. (2012).

Monsalve, M.L., Rodriguez, G.I., Mendez, R.A., Bernal, N.F.: Geology of the Well Nereidas 1, Nevado Del Ruiz Volcano, Colombia. Geothermal Resources Council Transactions, 22. (1998).

Moreno, D., Lopez-Sanchez, J., Blessent, D., Raymond, J.: Fault characterization and heat-transfer modeling to the Northwest of Nevado del Ruiz Volcano. Journal of South American Earth Sciences.. pp. 50-63. (2018).

Rojas, O.E.: Contribución al Modelo Geotérmico Asociado al Sistema Volcánico Nevado del Ruiz-Colombia, por Medio del Análisis de la Relación entre la Susceptibilidad magnética, Conductividad Eléctrica y Térmica del sistema, Universidad Nacional de Colombia – Master Thesis, (2012).

Saxena, V., Krief, K., and Adam, L.: Handbook of borehole acoustics and rock physics for reservoir characterization. Elsevier. pp. 349. (2018).

Tapias, J., Ramírez, N. E. M., Meléndez, M. F. A., Gutiérrez, F. A. A., Montoya, C. A. M., and Diederix, H. Geological map of colombia 2015. Episodes, 40(3). pp. 201-212. (2017).

Vargas, C.A., Koulakov, I., Jaupart, C., Gladkov, V., Gomez, E., Khrepy, S., and Al-Arifi, N. Breathing of the Nevado del Ruiz Volcano reservoir, Colombia, inferred from repeated seismic tomography. Sci. Rep. 7:46094. (2017).

Vélez, M. I., Blessent, D., Córdoba, S., López-Sánchez, J., Raymond, J., Parra-Palacio, E.: Geothermal potential assessment of the Nevado del Ruiz Volcano based on rock thermal conductivity measurements and numerical modeling of heat transfer. Journal of South American Earth Sciences. pp 153-164. (2018).

Proceedings 43rd New Zealand Geothermal Workshop
23-25 November 2021
Wellington, New Zealand
ISSN 2703-4275